

Dielectronic Recombination of Heliumlike Nickel

D. A. Knapp, R. E. Marrs, M. A. Levine,^(a) C. L. Bennett, M. H. Chen, J. R. Henderson, M. B. Schneider, and J. H. Scofield

Lawrence Livermore National Laboratory, Livermore, California 94550

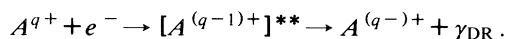
(Received 5 December 1988)

The dielectronic recombination excitation function for He-like Ni²⁶⁺ ions has been measured. The Ni²⁶⁺ ions were created and held in an electron-beam ion trap, and K x rays were detected. Several features were observed, including resonant excitation of Ni²⁶⁺ x rays and the transition from dielectronic recombination to direct excitation at threshold. The cross section for the KLL dielectronic recombination resonances relative to radiative recombination has been measured, and agrees with theoretical cross sections calculated using the multiconfiguration Dirac-Fock model.

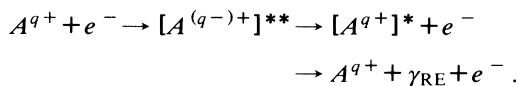
PACS numbers: 34.80.Kw, 32.80.Hd, 52.25.Nr

Dielectronic recombination (DR) is an important process in hot plasmas, affecting the ionization balance, emitted x-ray spectrum, and kinetics of the plasma. In recent years colliding-beam DR cross-section measurements have begun to appear for low ionization stages. These measurements involve $\Delta n = 0$ transitions in open-shell ions with transition energies ≤ 100 eV.¹⁻⁵ However, no measurements of DR cross sections have been made for higher ionization stages (such as He-like Fe²⁴⁺ or Ni²⁶⁺), which are produced in tokamaks^{6,7} and solar flares.⁸ For these ions, the most significant excitations are for $\Delta n \geq 1$, and therefore require a much higher interaction energy. An analogous process, resonant transfer and excitation in ion-atom collisions, has been measured (for K-shell excitations) in ions with net charge up to $q \approx 20$, with results in reasonable agreement with theory.^{9,10}

Dielectronic recombination occurs when an electron in the continuum is resonantly captured and produces a doubly excited state, followed by x-ray emission to a stabilized bound state:



The related process of resonant excitation (RE) occurs when the intermediate state decays by autoionization to an excited state, leaving the charge state of the ion unchanged. The excited state decays by x-ray emission:



RE can only occur for an incident electron energy greater than the direct excitation threshold for the x ray.

The resonance strengths for nonoverlapping DR resonances can be expressed in terms of the Auger and radiative widths of the resonances:

$$\begin{aligned} S(d, f) &\equiv \int_{-\infty}^{\infty} \sigma(d, f, E) dE \\ &= \frac{2\pi^2}{k_i^2} \frac{g_d}{2g_i} \frac{A_r(d \rightarrow f) A_A(d \rightarrow i)}{\sum A_r + \sum A_A}, \end{aligned}$$

where d and f refer to the resonant and final states, respectively, $\sum A_r$ and $\sum A_A$ are the total radiative and Auger widths, g_i and g_d are statistical weights for the initial and resonant states, respectively, and k_i is the incident electron wave number. For $\Delta n \neq 0$ transitions, $A_r \propto q^4$ for an isoelectronic sequence, while the Auger widths remain roughly constant as a function of ion charge q . For $q \approx 20$, A_r and A_A become comparable in size, making this region a particularly interesting one to study.

In the present experiment, the He-like Ni²⁶⁺ ions were held in the electron-beam ion trap (EBIT) at LLNL. This apparatus traps highly charged ions in the space charge of an electron beam, which also serves to ionize, excite, and recombine with them. EBIT is described in more detail elsewhere.^{11,12} The DR excitation function was measured by detecting the [Ni²⁵⁺]^{**} K x rays emitted at 90° to the electron beam direction with a planar Ge detector. For He-like target ions, exactly one K x ray is produced per DR, so, for a static ionization balance, the number of K x rays observed at a given beam energy is proportional to the DR cross section at that energy. This technique was first used by Briand *et al.* with an electron-beam ion source from which an x-ray signal from DR of Ar¹⁴⁺ was observed.¹³

On resonance, the DR cross section for Ni²⁶⁺ target ions is larger than the ionization cross section for Ni²⁵⁺ target ions, so setting the beam energy to a DR resonance will destroy the initial He-like charge state. An electron energy timing pattern designed to minimize this effect was used. After injection of low-charge-state ions into the trap, the electron beam energy was set to an "ionization energy" of 10 keV, at which no DR or RE occurred and the fraction of He-like ions was maximized. After a delay of 300 ms, in which the ionization balance came to equilibrium, the electron energy was dropped to the "probe energy" for a short time (typically between 4 and 16 ms), and the DR x rays were observed. The beam current was adjusted in proportion to the electron velocity to maintain a constant beam space charge in the trap. After the probe time, the beam energy was

changed back to the ionization energy for a time long enough to allow the charge-state balance to recover (typically about 70 ms). The probe-and-reionization cycle was repeated many times for each data run. An excitation function was constructed by taking data runs at different probe energies. The $n=2 \rightarrow 1$ direct excitation x rays from the common ionization energy provided a monitor of the number of Ni ions in the trap.

Typical spectra taken at the ionization energy and on and off resonance are shown in Fig. 1. The background of non-DR x rays seen in Fig. 1(c) comes from radiative recombination (RR) and from contamination of the trap with elements other than Ni; however, both these effects contribute a background of less than 1% of the peak signal. The $n=2 \rightarrow 1$ and $n=3 \rightarrow 1$ x rays are well separated from each other and from the higher members of the K series. Therefore, we present separate excitation functions for these three energy bands in Fig. 2. We use the usual Auger notation to label the various resonances; the *KLL* resonances, for example, have an intermediate state in which an electron is captured into the *L* shell and another is excited from the *K* shell to the *L* shell.

Three interesting features that have never before been directly observed are apparent in these data. First, the centroid of the $n=2 \rightarrow 1$ component of the *KLM* resonance feature is at a higher energy than the centroid of the $n=3 \rightarrow 1$ component, reflecting the different distribution of resonance strength for the two decay channels. Second, the intensity of the x rays in the $n \geq 4 \rightarrow 1$ ener-

gy band shows a sudden drop at the $n=2 \rightarrow 1$ direct excitation threshold, corresponding to the change from an electron bound in a high Rydberg level to a free electron. Third, the RE process is evident in the dominance of the $n=2 \rightarrow 1$ radiative decay channel for the *KMM* resonances. RE is particularly interesting because the Li-like *KMM* intermediate states can either Auger decay to the He-like $n=2$ states, yielding an $n=2 \rightarrow 1$ x ray, or they can radiatively decay, usually yielding an $n=3 \rightarrow 1$ x ray. For the *KMM* and *KMN* resonances, our data show a larger signal in the $n=2 \rightarrow 1$ channel than in the $n=3 \rightarrow 1$ channel, implying that the *L*-shell Auger rate is larger than the radiative decay rate for these resonances. It has been pointed out¹⁴ that the RE enhancement of $n=2 \rightarrow 1$ x-ray lines will be even larger for lower-*Z* elements since $A_r \propto q^4$, while the Auger rates remain roughly constant.

We now present a detailed comparison of experimental results and theoretical predictions for the *KLL* DR resonances. In the theoretical calculations, the atomic energy levels and bound-state wave functions were calculated using the multiconfiguration Dirac-Fock (MCDF) model in the extended average-level scheme. The effects of quantum-electrodynamic corrections, finite nuclear size, and relaxation were included in the calculations of the transition energies. The detailed relativistic Auger and radiative rates for each autoionizing state were calculated using first-order perturbation theory. Any possible

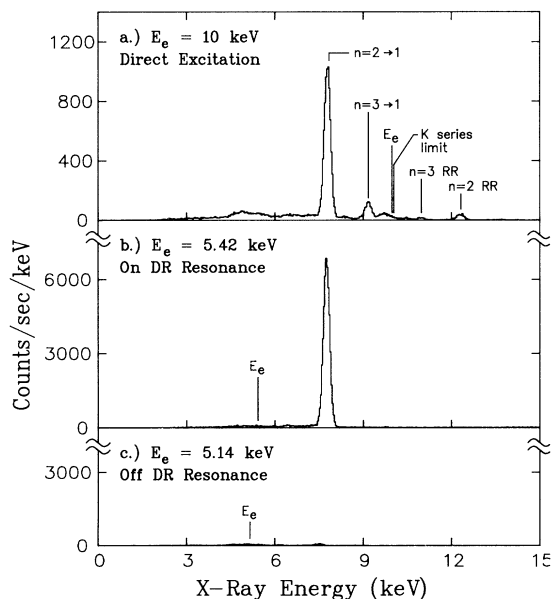


FIG. 1. Typical x-ray spectra taken with a Ge detector at different electron beam energies E_e : (a) at the ionization energy (10 keV), (b) on *KLL* resonance (5.42 keV), (c) off resonance (5.14 keV).

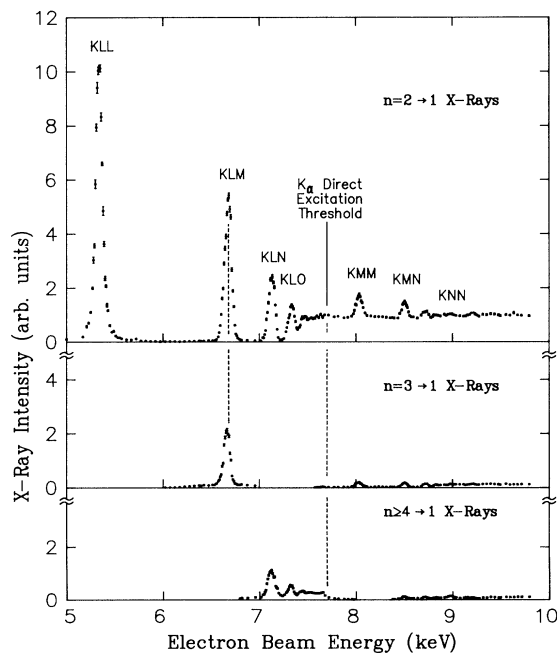


FIG. 2. Dielectronic recombination excitation function of Ni^{26+} target ions for three separate x-ray bands. Note that the cross section for $n=2 \rightarrow 1$ x rays merges smoothly into the impact-excitation cross section at the $K\alpha$ threshold.

angular correlation between the x-ray emission and the incident electron beam was neglected. Because the DR resonances have much narrower widths than the beam resolution, they were treated as δ functions normalized to the energy-averaged cross sections as defined by Lagattuta and Hahn.¹⁵ There are sixteen *KLL* DR resonant states from $1s2s^2$, $1s2s2p$, and $1s2p^2$ configurations, of which eight make sizable contributions to the DR cross section. The dominant contribution is from the $1s2p^2 D_J$ ($J = \frac{3}{2}, \frac{5}{2}$) states. A more complete presentation of the techniques used in these calculations is given in Ref. 16.

The data were first corrected for instrumental dead time and the charge-state depletion that occurred during the observation of DR. We measured the x-ray yield for various combinations of probe time, ionization time, and beam energy to determine the depletion and reionization rates. The largest correction applied was about 10%, for a probe energy at which the depletion was directly measured, so any systematic error from this procedure is small.

The number of ions in the trap and the ion-beam overlap cannot be measured directly, so an absolute measurement of the cross section is impossible. Instead, we normalize to RR for the same target ions at energies just above and below the DR resonances, using a technique similar to that of our electron-impact excitation studies.¹² The theoretical RR cross sections were calculated using a relativistic distorted-wave code.¹⁷ The $n=2$ RR cross sections used for the He-like charge state were $d\sigma/d\Omega(90^\circ) = 7.01$ b/sr at $E_e = 5.2$ keV and 6.03 b/sr at $E_e = 5.7$ keV. The estimated Ni charge-state distribution in the trap was used to extract the contribution of He-like ions to the observed RR x-ray intensity, as shown in Fig. 3. The systematic error introduced by this procedure is small, since the total contribution from non-He-like charge states is less than 15%, and both the

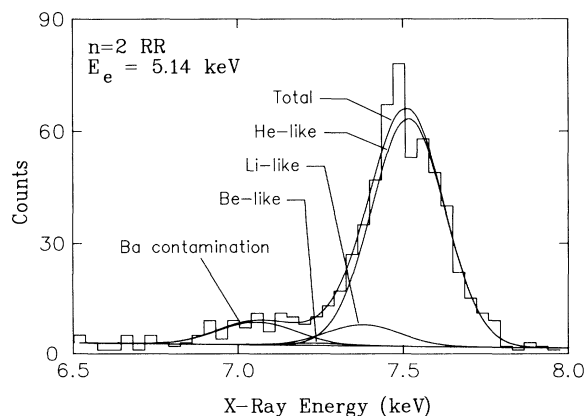


FIG. 3. Fit of the radiative recombination feature in a typical x-ray spectrum. The charge-state distribution was estimated from a fit to the shape of the *KLL* DR resonance peak. A background peak appears from RR of Ba ions in the trap.

RR and DR cross sections do not vary dramatically with charge state.^{16,17}

The electron beam energy distribution and Ni charge-state distribution were estimated from a fit of the experimental data with the relative theoretical DR resonance strengths for each charge state. The fitted beam energy distribution was a 54-eV-FWHM Gaussian. An independent measurement of this width was performed by placing a Kr gas cell in front of the detector and varying the electron beam energy so that RR x rays from H-like Ni disappeared under the Kr *K* edge. The preliminary results of this measurement (57 ± 5 eV FWHM) are consistent with the results of the DR fit. An electron energy offset of 77 eV was applied to the data to match the theoretical resonance energies, which can be calculated to very high accuracy. This offset is consistent with the estimated size of the space-charge potential from ions in the trap, and in agreement with the energy offset derived from the fit to the RR x rays.

The validity of the analysis procedure was tested by analyzing excitation functions taken with different beam currents, probe times, and initial charge-state distributions. All gave consistent results. Data taken with a probe beam current of 74 mA are shown in Fig. 4, together with the theoretical DR resonance strengths convoluted with the beam energy distribution. The apparent excess cross section at higher electron beam energies results from non-He-like Ni charge states in the trap. Excitation functions taken with a smaller He-like charge fraction showed larger DR signals at the energies predicted for lower charge states.

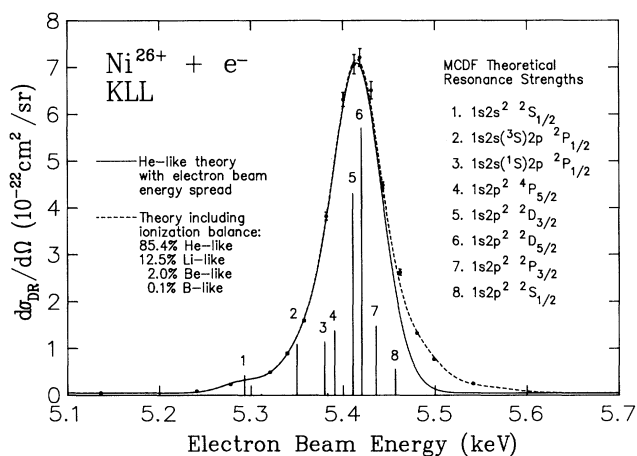


FIG. 4. Comparison of experiment and theory for the *KLL* dielectronic recombination feature. The stick diagram shows the locations and relative amplitudes of the calculated resonances for the He-like target ions. The curves are the theoretical resonance strengths folded with the electron beam energy distribution (solid: He-like only; dashed: estimated charge-state distribution). The systematic error in the normalization of the data is 11%.

The overall normalization uncertainty in the determination of the cross sections from comparison with the RR x rays is estimated to be 11%, including a 3% uncertainty in the theoretical RR cross sections. Measurements of the relative ion-beam overlap at electron energies just above and below the *KLL* resonance showed a reproducible change over the energy interval. Since the origin of this effect is not well understood, the average value was used and the entire difference included in the quoted uncertainty. The total DR resonance strength in the *KLL* resonances for He-like Ni target ions, correcting for non-He-like charge states, is measured as $(6.8 \pm 0.8) \times 10^{-19} \text{ cm}^2 \text{ eV}$.

In conclusion, we have demonstrated a powerful new technique for the measurement of dielectronic recombination in highly charged ions, and have made the first direct measurement of DR for $\Delta n \geq 1$, providing an accurate measurement of the summed *KLL* resonance strength and some information about the distribution of the resonance strength. This technique allows the detailed study of all radiative electron-ion excitations in highly charged ions.

We wish to thank J. Gier, A. Hinz, D. Nelson, and D. Phillips for their assistance in these measurements. We thank R. J. Fortner for his encouragement and support. This work was performed under the auspices of the U.S. Department of Energy at the Lawrence Livermore National Laboratory under Contract No. W-7405-Eng-48.

^(a)Permanent address: Lawrence Berkeley Laboratory, Berkeley, CA 94720.

¹J. B. A. Mitchell, C. T. Ng, J. L. Forand, D. P. Levac, R. E. Mitchell, A. Sen, D. B. Miko, and J. Wm. McGowan, Phys. Rev. Lett. **50**, 335 (1983).

²D. S. Belić, G. H. Dunn, T. J. Morgan, D. W. Mueller, and C. Timmer, Phys. Rev. Lett. **50**, 339 (1983).

³J. F. Williams, Phys. Rev. A **29**, 2936 (1984).

⁴A. Müller, D. S. Belić, B. D. DePaola, N. Djurić, G. H. Dunn, D. W. Mueller, and C. Timmer, Phys. Rev. Lett. **56**, 127 (1986).

⁵P. F. Dittner, S. Datz, R. Hippler, H. F. Krause, P. D. Miller, P. L. Pepmiller, C. M. Fou, Y. Hahn, and I. Nasser, Phys. Rev. A **38**, 2762 (1988).

⁶F. Bombarda, R. Gianella, E. Källne, G. J. Tallents, F. Bely-Dubau, P. Faucher, M. Cornille, J. Dubau, and A. H. Gabriel, Phys. Rev. A **37**, 504 (1988).

⁷H. Hsuan, M. Bitter, K. W. Hill, S. von Goeler, B. Grek, D. Johnson, L. C. Johnson, S. Sesnic, C. P. Bhalla, K. R. Karim, F. Bely-Dubau, and P. Faucher, Phys. Rev. A **35**, 4280 (1987).

⁸K. Tanaka, T. Watanabe, K. Nishi, and K. Akita, Astrophys. J. **254**, L59 (1982).

⁹J. A. Tanis, Nucl. Instrum. Methods Phys. Res., Sect. A **262**, 52 (1987).

¹⁰M. Schulz, E. Justiniano, R. Schuch, P. H. Mokler, and S. Reusch, Phys. Rev. Lett. **58**, 1734 (1987).

¹¹M. A. Levine, R. E. Marrs, J. R. Henderson, D. A. Knapp, and M. B. Schneider, Phys. Scr. **T22**, 157 (1988).

¹²R. E. Marrs, M. A. Levine, D. A. Knapp, and J. R. Henderson, Phys. Rev. Lett. **60**, 1715 (1988).

¹³J. P. Briand, P. Charles, J. Arianer, H. Laurent, C. Goldstein, J. Dubau, M. Loulergue, and F. Bely-Dubau, Phys. Rev. Lett. **52**, 617 (1984).

¹⁴P. Faucher and J. Dubau, Phys. Rev. A **31**, 3672 (1985).

¹⁵K. LaGattuta and Y. Hahn, J. Phys. B **15**, 2101 (1982).

¹⁶M. H. Chen, Phys. Rev. A **33**, 994 (1986).

¹⁷E. B. Saloman, J. H. Hubbell, and J. H. Scofield, At. Data Nucl. Data Tables **38**, 1 (1988).